THE JOURNAL OF PHYSICAL CHEMISTRY A

Article

pubs.acs.org/JPCA

Structural Influences on Preferential Oxazolone versus Diketopiperazine b_2^+ Ion Formation for Histidine Analogue-Containing Peptides

Ashley C. Gucinski,[†,§] Julia Chamot-Rooke,[‡] Edith Nicol,[‡] Árpád Somogyi,[†] and Vicki H. Wysocki*[,†]

[†]Department of Chemistry and Biochemistry, The University of Arizona, 1306 East University Boulevard, Tucson, Arizona 85721, United States

[‡]Department de Chimie, Laboratoire des Mécanismes Réactionnels, École Polytechnique, 91120 Palaiseau, France

Supporting Information

ABSTRACT: Studies of peptide fragment ion structures are important to aid in the accurate kinetic modeling and prediction of peptide fragmentation pathways for a given sequence. Peptide b_2^+ ion structures have been of recent interest. While previously studied b_2^+ ions that contain only aliphatic or simple aromatic residues are oxazolone structures, the HA b_2^+ ion consists of both oxazolone and diketopiperazine structures. The structures of a series of histidine-analogue-containing Xxx-Ala b_2^+ ions were studied by using action infrared multiphoton dissociation (IRMPD) spectroscopy, fragment ion hydrogen−deuterium exchange (HDX), and density functional theory (DFT) calculations to systematically probe the influence of different side chain structural elements on the resulting b_2^+ ion structures formed. The b_2^+ ions studied include His−Ala (HA), methylated histidine analogues, including π-methyl-HA and τ-methyl-HA, pyridylalanine (pa) analogues, including 2-(pa)A, 3-(pa)A, and 4-(pa)A, and linear analogues, including diaminobutanoic acid−Ala (DabA) and Lys−Ala (KA). The location and accessibility of the histidine π-nitrogen, or an amino nitrogen on an aliphatic side chain, were seen to be essential for diketopiperazine formation in addition to the more typical oxazolone structure formation, while blocking or removal of the τ-nitrogen did not change the b_2^+ ion structures formed. Linear histidine analogues, DabA and KA, formed only diketopiperazine structures, suggesting that a steric interaction in the HisAla case may interfere with the complete trans−cis isomerization of the first amide bond that is necessary for diketopiperazine formation.

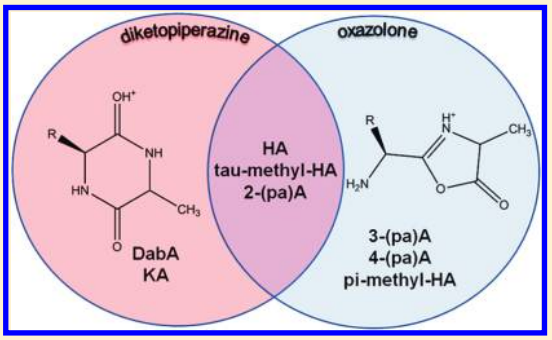

INTRODUCTION

Elucidation of structural influences on chemical reactions, including unimolecular dissociation reactions, is critical to understanding many chemical and biochemical processes. This is of special interest in the field of protein characterization through bottom-up proteomics, where peptide fragmentation spectra are used to identify proteins from complex mixtures. In peptide mass spectrometry, protonated peptides are generally fragmented by activating via collisions with a gaseous target to cause collision-induced dissociation (CID), which causes characteristic peptide fragmentation at the amide bond between amino acid residues. Fragment ions produced by a given activation method then provide sequence information through the ion types produced (e.g., N-terminal b and C-terminal y ions).[1] The peptide fragmentation spectra are analyzed by peptide/protein identification algorithms. These algorithms compare experimental spectra to theoretical peptide spectra (or peak lists) generated from databases of protein sequences to identify the peptide sequence associated with the MS/MS spectrum. However, this approach is not without error; in fact, only a relatively small percentage of the peptide fragmentation spectra are correctly matched to peptide sequences.[2−4]

Many reasons exist to explain the discordance between the number of peptide MS/MS spectra generated and the number assigned to peptide sequences. First, only a small amount of chemical information is incorporated into the models used to generate the theoretical spectra. The simplified models of the peptide fragmentation process used by most peptide identification algorithms do not include nonstandard fragmentation pathways, including sequence scrambling as was reported by Paizs and co-workers, or the presence of isobaric nonstandard fragments, including the presence of non-C-terminal water loss, which was first reported by Gaskell and co-workers and more recently presented by Wysocki and co-workers for the model peptide system YAGFL.[5−8] Additionally, currently available algorithms do not take full advantage of peptide fragment ion intensity information. Intensity enhancement can suggest preferential formation of certain fragment ions, providing additional certainty of the peptide sequence identification;[9] without the incorporation of intensity, this information is

Received: January 9, 2012
Revised: March 20, 2012
Published: March 26, 2012

dx.doi.org/10.1021/jp300262d | J. Phys. Chem. A 2012, 116, 4296−4304

merely lost in the peptide identification process. Similarly, not all peptide fragment sequencing ions for a given peptide sequence will be present in the MS/MS spectrum. The absence or enhancement of specific peptide fragment ions in an MS/MS spectrum can give additional information and confidence in the sequence identification.

Residue-specific preferential fragmentation behavior has been studied extensively for a variety of amino acids, including histidine, aspartic acid, and proline.[10−18] Factors such as sterics, proton mobility, size, conformation, charge state, and residue composition have been related to the distinct fragmentation patterns of specific peptide sequences.[19−27] Several studies have focused on the preferential fragmentation behavior of histidine. Wysocki and co-workers used a data mining approach to examine a set of doubly charged tryptic peptides, which identified that preferential cleavage was more likely to occur for histidine than for any other residue.[28] The preferential cleavage is likely attributed to the ability of the histidine side chain to serve as a protonation site, which would facilitate fragmentation at the position C-terminal to the histidine residue, in accordance with the mobile proton model and charge-directed fragmentation behavior.[19] Using a series of angiotensin and angiotensin analogues, Tsaprailis et al. examined the mechanism of the enhanced cleavage occurring C-terminal to histidine residues.[17] The enhanced intensity of the fragments resulting from cleavage C-terminal to the histidine residue was attributed to the involvement of the protonated side chain in a proton transfer event that facilitated fragmentation. The unique properties of histidine in peptides and proteins are of interest not only in the field of peptide mass spectrometry but also throughout biology and chemistry. The imidazole side chain allows for histidine to participate in a wide variety of chemical processes, including metal binding, phosphorylation, pH regulation, and involvement in enzyme-active site interactions.[29]

One explanation for the unique fragmentation behavior displayed by histidine is that histidine has the potential to generate an alternative fragment ion structure with the involvement of the imidazole side chain. Both the O'Hair and Wysocki laboratories have investigated the structures of histidine-containing b_2^+ ions. O'Hair and co-workers used density functional theory (DFT) calculations in combination with MS/MS spectra fragmentation patterns to examine the structures of the Gly−His and His−Gly b_2^+ ion systems.[30] When compared to the fragmentation pattern of a synthetic (cyclic) diketopiperazine GH peptide, excellent agreement was seen in both the MS/MS spectra and the DFT calculations.[15] As the diketopiperazine was also found to be thermodynamically favored in comparison to the oxazolone structure, the assignment of the diketopiperazine structure for both the HG and GH systems was supported. Similarly, Perkins et al. investigated the structure of the HA b_2^+ ion by using action IRMPD spectroscopy, fragment ion hydrogen−deuterium exchange (HDX), and DFT calculations.[15] Results from the action IRMPD spectroscopy experiment, a direct method to identify the structural features of the ion, confirmed the presence of IR stretches corresponding to both oxazolone and diketopiperazine structures for the HA b_2^+ ion. Despite being an indirect structural method, the HDX experimental results were in agreement with the IRMPD spectroscopy data. The HA b_2^+ ion featured a bimodal exchange distribution, reflecting the presence of two ion structures: a rapidly exchanging oxazolone, incorporating three deuterium atoms, and a more slowly exchanging diketopiperazine structure, incorporating one deuterium atom.

Knowledge of peptide fragment ion structure is essential for accurate kinetic modeling of the fragmentation process. Because different fragment ion structures are formed as a result of different fragmentation pathways, the fragment ion structures provide information about which pathways need to be incorporated into a kinetic model of fragmentation for a given peptide sequence. An improved knowledge of the ion structure and corresponding mechanism of formation may improve the success of kinetic-model-based peptide identification algorithms developed by several groups. The HA system presents a unique situation, as the only reported structure to date that produces two different b_2^+ fragment ion structures. Other b_2^+ ion structures previously reported have contained only aliphatic or aromatic residues and feature only oxazolone b_2^+ ion structures.[31−33] In contrast to results for b_2^+ ions, other groups, including the Polfer laboratory,[34−36] have reported examples of large b fragment ions featuring a mixture of b ion structures.

On the basis of the results seen for the HA b_2^+ ion system, we proposed that the availability of the basic histidine side chain provides an alternative protonation site for the ionizing proton, leaving the N-terminal amine free to serve as a nucleophile in formation of the diketopiperazine structure. In order to identify which structural elements of the histidine side chain are essential for the formation of a diketopiperazine versus an oxazolone b_2^+ ion structure, the structures of a series of histidine analogue-containing b_2^+ ions were studied to systematically probe which structural elements influence the resulting b_2^+ ion structure(s) formed. Fragment ion gas-phase HDX, variable wavelength action IRMPD spectroscopy, and DFT calculations were used in combination in order to elucidate information about the ion structure. Ultimately, these studies can help to provide a more complete understanding of structural influences on fragmentation pathways.

EXPERIMENTAL METHODS

Precursor pentapeptides were synthesized in-house using standard solid phase peptide synthesis protocols.[37] Non-standard Fmoc-protected amino acid analogue residues (2-pyridylalanine, 3-pyridylalanine, and 4-pyridylalanine, designated as 2-(pa), 3-(pa), and 4-(pa), respectively) were obtained from CSPS Pharmaceuticals (San Diego, CA). Methylated Fmoc-protected histidine residues were obtained from Sigma Aldrich (St. Louis, MO). Standard Fmoc-protected residues were obtained from EMD Biosciences (Gibbstown, NJ). The structures of all histidine-analogue residues studied are shown in Figure 1. Solid peptides were diluted in 50:50:0.1% water/acetonitrile/formic acid to a concentration of approximately 10 μM prior to mass spectrometric analysis.

Action IRMPD spectroscopy experiments were performed at the CLIO free electron laser facility (Orsay, France), as developed and described previously by Maitre, Ortega, and co-workers.[38−40] Briefly, protonated peptide precursors were generated via electrospray ionization and introduced into a modified Bruker Esquire 3000+ Paul-type ion trap mass spectrometer. Peptides were fragmented by using collision-induced dissociation with argon and isolated in the ion trap prior to fragmentation using the tunable wavelength CLIO free electron laser. Fragmentation is achieved when the frequency of the laser matches the vibrational frequency of the bonds in the ion, allowing for absorption of photons in excess of the bond

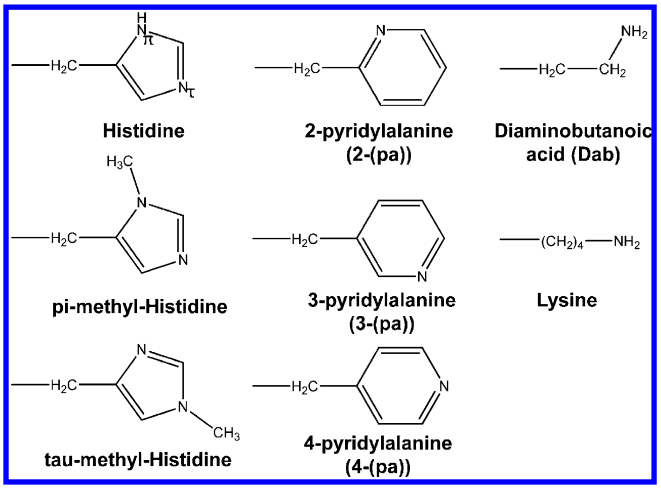

Figure 1. Structures of histidine side chain analogues studied via IRMPD spectroscopy and fragment ion hydrogen−deuterium exchange. All b_2^+ ions studied featured alanine as the second residue.

dissociation energies of the ion. The relative ratio between the fragment ion and precursor ion intensity was used to generate the action IRMPD spectrum, which is plotted as fragment:-precursor ion intensity ratio versus laser frequency in wavenumbers. Action IRMPD spectra were acquired over the range of approximately 1050 to 2050 cm^{-1} at a stepsize of 4 cm^{-1}. As the power of the free electron laser was not uniform throughout the entire spectral range (most notably, the power was suppressed at the oxazolone stretch region of the spectrum), spectra were power corrected using laser power profile curves. A typical comparison between power-corrected and raw spectra is shown for the HA b_2^+ ion from the protonated HAAAA precursor in Supporting Information Figure S1.

Theoretical IR spectra were generated for comparison to action IRMPD spectra acquired at the CLIO FEL facility. Starting structures were generated via Monte Carlo Conformational Searching simulations using MacroModel (Schrodinger, Inc., Portland, OR). A subset of the generated structures were then optimized by using density functional theory calculations using the B3LYP hybrid functional with both the 6-31G and 6-311++G** basis sets using the Gaussian09 software package (Gaussian, Inc., Wallingford, CT).[41] The calculated harmonic vibrational frequencies were scaled with a factor of 0.98 and a Lorentzian curve was applied to generate a FWHM resolution of 10 cm^{-1} for each absorption calculated.

Fragment ion hydrogen−deuterium exchange (HDX) experiments were performed using a Bruker Apex Qh 9.4T FTICR mass spectrometer (Bruker Daltonics, Billerica, MA). Protonated peptides were generated by using electrospray ionization. Peptides were fragmented by using quadrupole (eV) CID and all ions, fragment and precursor, were simultaneously transferred into the ICR cell, where they were allowed to react with perdeuterated methanol (CD_3OD, Cambridge Isotope Laboratories, Andover, MA) for a variety of different pulse (HDX reaction) time lengths to examine the exchange profiles, including the extent of exchange and relative exchange rates, for the ions in the gas phase.

RESULTS AND DISCUSSION

The HA b_2^+ ion has been reported previously to feature both oxazolone and diketopiperazine structures.[15] We propose that these distinct b_2^+ ion structures are formed via different intermediates: the diketopiperazine requires the cis conformation of the first amide bond to facilitate nucleophilic attack by the N terminus, whereas the oxazolone requires the trans conformation of the amide bond to facilitate nucleophilic attack by the first carbonyl oxygen.[42] It is reasonable to assume that the two distinct b_2^+ ion structures might fragment via different fragmentation pathways, with certain fragments present only for the oxazolone structure and not the diketopiperazine, or vice versa. To determine if specific IRMPD fragment ions reflect either b_2^+ ion structure exclusively, the action IRMPD spectrum of the HA b_2^+ ion was generated independently from each fragment observed in the action IRMPD experiment, as shown in Supporting Information Figure S2. Theoretical IR spectra for the lowest-energy diketopiperazine and oxazolone HA b_2^+ ion structures are shown in Supporting Information Figure S3 for comparison.[15] As shown in the theoretical spectra, the diketopiperazine structure features three strong characteristic stretches at approximately 1620, 1690, and 1750 cm^{-1}, which correspond to the histidine imidazole ring breathing mode, the simultaneous stretching of the protonated histidine ring breathing mode and the bridging diketopiperazine amide C═O stretch, and the unprotonated amide I C═O stretch, respectively; the oxazolone structure features a characteristic stretch at approximately 1875 cm^{-1}, corresponding to the ring C═O stretch. Spectra for each individual fragment m/z of the HA b_2^+ ion reflect mixtures of oxazolone and diketopiperazine structures, with the largest contribution to the oxazolone ring C═O stretch coming from the m/z 181 (CO loss) ion, as expected from previous literature identifying CO loss from oxazolones.[43] The IRMPD spectra of the HA b_2^+ ion and protonated cyclic HA have been shown previously to yield the same fragment ions (m/z 110, 164, 166, 181, and 192) but in varied intensities.[44] While the diketopiperazine and oxazolone structures are different, the small size and limited chemical loss combinations of the ions may limit the number of energetically favorable fragmentation pathways available. Additionally, interconversion between the isomers may also occur during the (slow-heating trap CID) fragmentation process although there is a large energy difference between the isomers, and the oxazolone isomer is always the more minor isomer present based on HDX and IRMPD experiments. Differences in IRMPD fragmentation pathways alone cannot be used to distinguish between the preferential formation of oxazolone versus diketopiperazine for this system.

Proton location has been shown, in certain circumstances, to have a great effect in determining the possible pathways of peptide fragmentation.[19,45] The lowest-energy HA b_2^+ ion diketopiperazine and oxazolone structures are protonated on the histidine side chain imidazole ring π-nitrogen, with the ionizing proton bridging with other functional groups in the ion. This protonation site is consistent with that seen by Lucas and co-workers for the alanylhistidine dipeptide.[46] Although final location of the proton in the product ion does not necessarily indicate location of the proton during ring closure and fragmentation, it is of interest to determine if both the location and availability of the π-nitrogen for protonation are essential for the formation of both the diketopiperazine and oxazolone structures. To probe the influence of the availability of the π-nitrogen for protonation on the formation of diketopiperazine or oxazolone product ions, the structure of the b_2^+ ion formed from the π-methyl-HAAAA protonated precursor was studied. Methylation blocks the nitrogen,

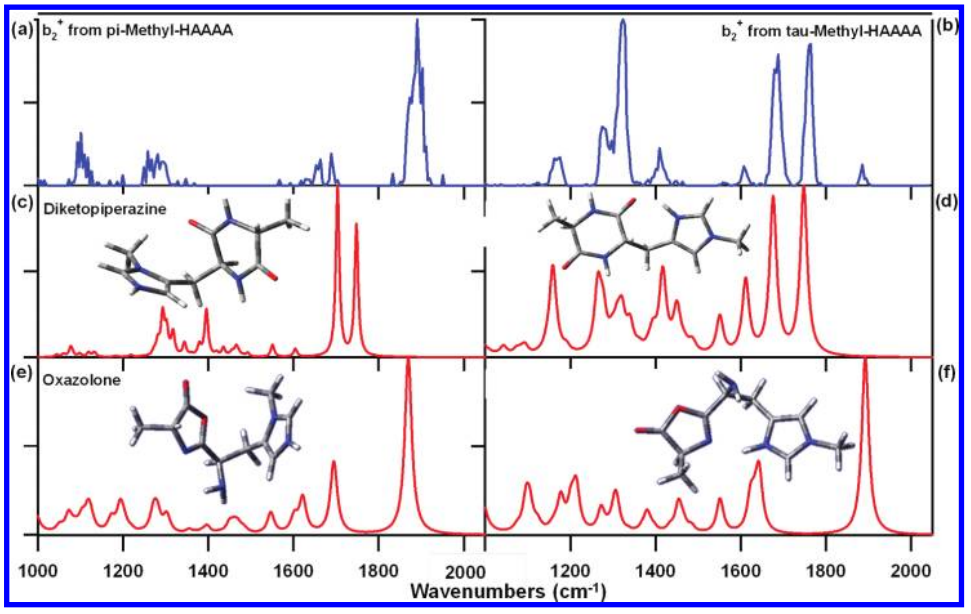

Figure 2. Experimental action IRMPD spectra for the (a) π-methyl-HA and (b) τ-methyl-HA b_2^+ ions. Corresponding lowest-energy calculated spectra are shown below the experimental spectra in panels c through f. The enhanced stretch at approximately 1340 cm^{-1} is present in greater intensity than that predicted in the experimental spectrum, consistent with that previously reported for the HA b_2^+ ion experimental spectrum,[15] and corresponds to several C−H stretches in the molecule.

preventing it from being a site of protonation or proton bridging. To compare the effect of methylation of the π-nitrogen with that of the τ-nitrogen, the structure of the b_2^+ ion from the τ-methyl-HAAAA precursor was also studied. The action IRMPD spectra for the π-methyl-HA and τ-methyl-HA b_2^+ ions are shown in Figure 2, while the HDX results for the corresponding b_2^+ ions are shown in Figure 3. Optimized

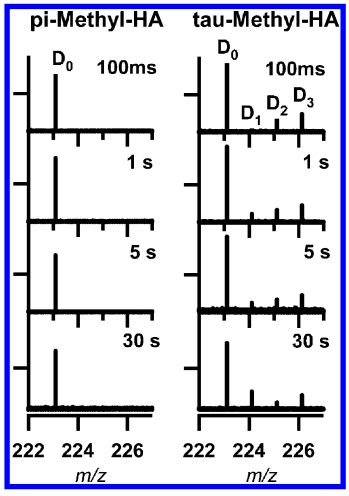

Figure 3. Fragment ion HDX for methyl-substituted histidine side chain analogues. Exchange behavior at four different time points (100 ms, 1 s, 5 s, and 30 s) is shown.

lowest-energy structures from DFT calculations can be found superimposed on the corresponding theoretical spectra, with magnified structures and the *xyz* coordinates available in the Supporting Information.

Similar to the HA b_2^+ ion system, the IRMPD spectrum of the τ-methyl-HA b_2^+ ion (Figure 2b) features stretches indicating the presence of both oxazolone and diketopiperazine structures. Additionally, the HDX behavior for τ-methyl-HA (Figure 3, right) shows the initial incorporation of three deuterium atoms, indicative of the oxazolone structure, as well as a slowly exchanging D_1 population, characteristic of a diketopiperazine structure. Methylation at the τ-nitrogen, therefore, has no effect on either the HDX behavior of the system or on the ability to form multiple b_2^+ ion structures. As the formation of the diketopiperazine is not inhibited when the τ-nitrogen is methylated, the presence and/or availability of the τ-nitrogen is not essential for diketopiperazine formation. However, methylation of the histidine π-nitrogen in the π-methyl-HA system blocks formation of the diketopiperazine; the IR spectrum (Figure 2a) features stretches reflecting only an oxazolone structure, and no deuterium atoms were seen to incorporate into the π-methyl HA b_2^+ ion, even after long periods (up to 90 s) of interaction with the deuterating reagent. The availability and presumably the protonation of the π-nitrogen on the histidine side chain imidazole ring is necessary not only for the formation of the diketopiperazine structure in addition to the oxazolone structure but also in order for HDX to occur with CD_3OD, presumably by bridging the proton to another heteroatom so that CD_3OD insertion can occur to allow the relay mechanism of exchange.[47,48] With methylation at the π-nitrogen and protonation on the τ-nitrogen, sterically inhibiting any proton bridging between the imidazole ring and other heteroatoms, no HDX occurs.

In order to further probe the involvement of structural features of the histidine side chain in the formation of both diketopiperazine and oxazolone b_2^+ ion structures, several pyridylalanine residue-containing Xxx-Ala b_2^+ ions were studied. Pyridylalanine (pa) is a histidine analogue that has only one nitrogen in an aromatic six-membered ring. The increased ring size causes a slight change in the dihedral bond angles in the side chain ring (e.g., the Cα−Cβ−Nπ angle in histidine is 123.2 versus 117.3 for the 2-(pa) analogue). 2-(pa) maintains the same number of bonds between the peptide backbone and the ring nitrogen as in the case of the histidine π-nitrogen, whereas 3-(pa) resembles histidine if only the τ-nitrogen were present,

dx.doi.org/10.1021/jp300262d | J. Phys. Chem. A 2012, 116, 4296−4304

and 4-(pa) moves the nitrogen to the para position of the ring, an additional bond farther away from the peptide backbone relative to 3-(pa). Variable wavelength IRMPD spectra for all pyridylalanine structures are shown in Figure 4, and the corresponding HDX behaviors of the b_2^+ ions are shown in Figure 5.

The 2-(pa)A b_2^+ ion, the side chain analogue most similar to histidine with the π-nitrogen retained, behaves in the same manner as HA. The IR spectrum features diketopiperazine and oxazolone stretches, and HDX results reveal a population for both the diketopiperazine and oxazolone structure. However, when the side chain nitrogen is moved, an additional bond further from the backbone, somewhat equivalent to the histidine τ-nitrogen position, in the case of 3-(pa)A, both spectroscopy and HDX reflect the presence of a single oxazolone structure. (Strictly speaking, there is no exchange detected for this ion (see 3-(pa)A) but we provide an explanation below.) The intense oxazolone C═O ring stretch (~1885 cm^{-1}) is observed while the diketopiperazine amide stretch (~ 1760 cm^{-1}) is not. Note that the calculated stretch for the second diketopiperazine amide stretch at 1685 cm^{-1} overlaps with the oxazolone ring C═N stretch in the calculated oxazolone structure, so this peak is less useful for structural assignment than the absence of the peak at 1760 cm^{-1}; in either case, the absence of a band is less useful than its presence. In addition to the IR results, even at long HDX reaction times, the D_0 population is the only population present for the 3-(pa)A, again suggesting that it is necessary for the deuterating reagent to bridge or be present at the π-nitrogen location in order for exchange to occur. In the case of the 3-(pa)A b_2^+ ion, the nitrogen in 3-(pa) is too far away from other basic sites with which the deuterating reagent can react, therefore preventing the relay mechanism of deuterium incorporation from occurring. The results from 3-(pa)A suggest that the τ-nitrogen of histidine is not involved in the formation of the diketopiperazine structure for HA. The presence of a side chain nitrogen is insufficient to afford formation of both diketopiperazine and oxazolone structures. Instead, the availability and position of the π-nitrogen are essential for the formation of the b_2^+ ion structures that are dominant for HA and 2-(pa)A.

Structural characterization of the 4-(pa)A b_2^+ ion tests whether an even more remote para nitrogen position alters which b_2^+ ion structures are formed. The action IRMPD spectrum for the 4-pa(A) b_2^+ ion features a predominant oxazolone b_2^+ structure, similar to the results obtained for the 3-(pa)A system. Similarly to the 3-(pa)A system, little to no hydrogen−deuterium exchange is detected for the 4-(pa)A system, as the increased distance and change in orientation of the ring nitrogen away from the rest of the structure prevents successful bridging of the deuterated methanol in the relay

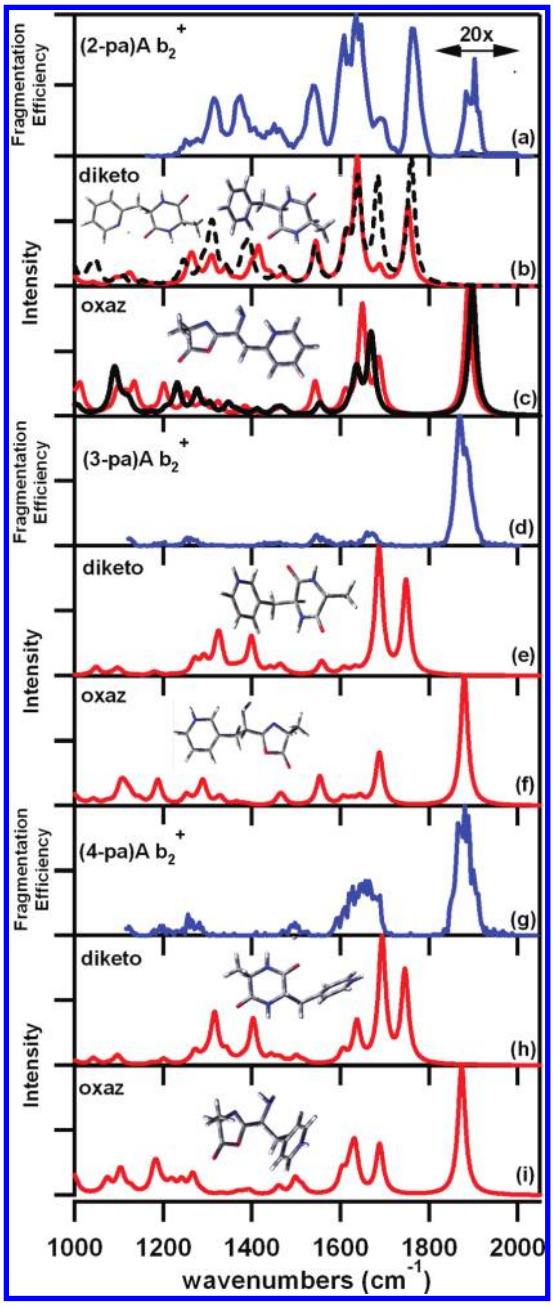

Figure 4. Experimental action IRMPD spectra of (a) (2-pa)A, (d) (3-pa)A, and (g) (4-pa)A b_2^+ ions. Corresponding lowest-energy theoretical diketopiperazine and oxazolone IR spectra are shown in red (and black) beneath each experimental spectrum. The dashed line in panel b denotes the second lowest-energy diketopiperazine structure (right), which likely also contributes to the overall spectrum, while the black line in panel c denotes the second lowest-energy oxazolone structure.

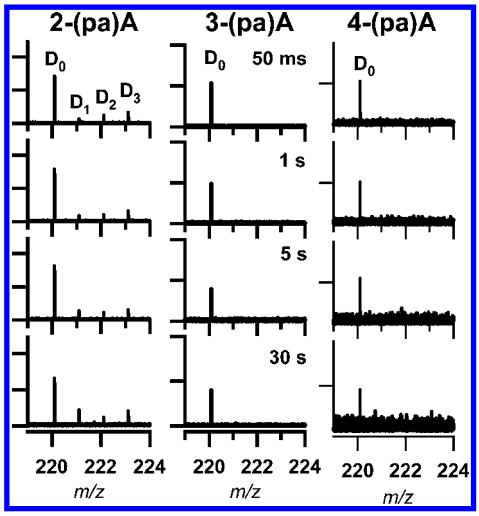

Figure 5. Fragment ion HDX of pyridylalanine-containing Xxx-Ala b_2^+ ions.

dx.doi.org/10.1021/jp300262d | J. Phys. Chem. A 2012, 116, 4296−4304

mechanism. On the basis of the results from the methylated histidine and pyridylalanine analogue b_2^+ ion systems, diketopiperazine formation can occur when the side chain ring nitrogen is at the delta (δ) position three bonds from the peptide backbone and at a C(O)−N−CHR−N dihedral angle of approximately 120°.

While the importance of the location and approximate dihedral angle of the π-nitrogen in the histidine side chain for diketopiperazine formation has been demonstrated, the need for the side chain nitrogen to be a component of a cyclic, aromatic side chain has not been explored. To determine if an aromatic, cyclic side chain is required for diketopiperazine formation, diaminobutanoic acid (Dab), which features an ethylamine side chain, as shown in Figure 1 (and typical aliphatic carbon dihedral angle of ∼109.5°) was substituted for histidine in the HA system. In comparison to histidine, incorporation of Dab removes any side chain bulk caused by the presence of the ring structure, while still providing an amino group at the δ position, the same number of bonds away from the peptide backbone as the π-nitrogen in the imidazole side chain ring. As shown in Figure 6, action IRMPD

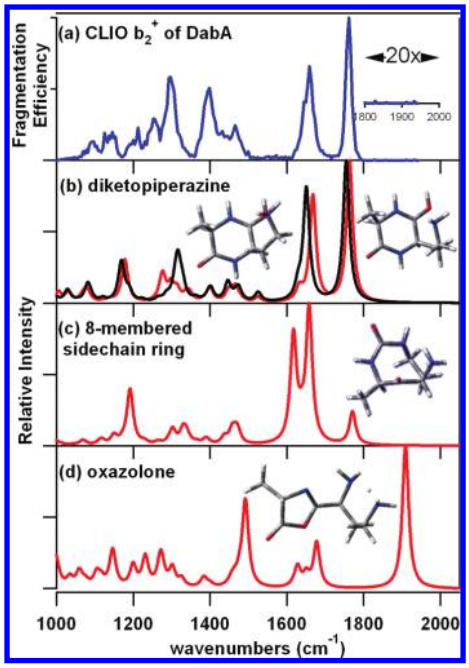

Figure 6. Experimental action IRMPD spectra for the (a) DabA b_2^+ ions. Theoretical IR spectra corresponding to the lowest-energy (b) side chain protonated diketopiperazine (the structure at left corresponds to the spectrum in black, at right to the spectrum in red), (c) 8-membered side chain ring, and (d) oxazolone structures are shown for comparison. The spectral region from 1800−2000 cm^{-1} is magnified 20-fold to clearly identify the absence of the oxazolone CO stretch. The enhanced stretch at ∼1390 cm^{-1} is consistent with that observed in the HA and τ-Me-HA b_2^+ ion systems, reflecting several C−H stretches in the molecule.[15].

spectroscopy of the DabA b_2^+ ion generated from the protonated pentapeptide precursor DabAAAA reflects only a dominant diketopiperazine structure with no measurable oxazolone CO stretch near 1900 cm^{-1}. In contrast to previous systems, the best spectral agreement with the experimental IR spectrum for DabA is not seen with the lowest-energy diketopiperazine structure, which is protonated on the side chain amine. Instead, best spectral agreement is seen for protonation on the Dab amide carbonyl oxygen producing a hydroxyimine tautomer, a structure that is 100.2 kJ/mol higher in energy than the side chain protonated diketopiperazine. If calculations are performed for the Dab b_2^+ ion protonated instead on the alanine carbonyl, the structure converts during the optimization calculation to the hydroxyimine tautomer, and the IR spectrum does not match the experimental spectrum (see Supporting Information). Strong overlap between the experimental spectrum and the calculated diketopiperazine/hydroxyimine IR spectrum is seen for both amide stretches at 1670 cm^{-1} and 1765 cm^{-1}, with the latter protonated at the carbonyl oxygen and charge-stabilized by the side chain amine. The DabA result is unique in that this is the first structure of the series reported here that produces the diketopiperazine exclusively. In results not presented in this article, we have also determined that His−Pro produces exclusively diketopiperazine b_2^+ ions.[49] While protonation at the Dab carbonyl oxygen may seem unusual in the presence of an amino group, the charge is stabilized by the side chain amino group; this is similar to the protonation pattern for His−Ala diketopiperazine and 2-(pa)Ala diketopiperazine, where a proton bridges from the sidechain to the carbonyl of the His or 2-(pa).

In addition to the spectroscopic data, the DabA b_2^+ ion HDX distribution, as shown in Figure 7a, reflects a dominant

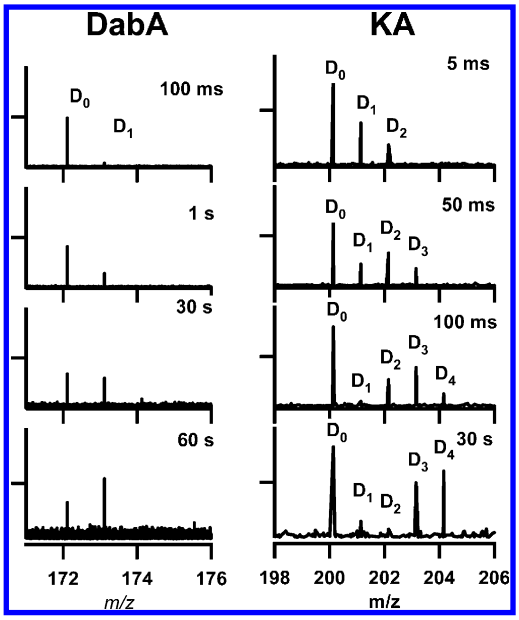

Figure 7. HDX of b_2^+ ions with acyclic histidine side chain analogues: (a) DabA and (b) KA at four different exchange time points in an FTICR HDX experimental setup.

population with one exchanging hydrogen. Previous diketopiperazine structures, including the HA diketopiperazine generated from the protonated HAAAA precursor, as well as the protonated synthetic diketopiperazine HA, have presented the ability to exchange one hydrogen for deuterium. While the Dab side chain has exchangeable hydrogens, the ability to incorporate only one deuterium may be a result of the limited length and geometric flexibility of the side chain, which interferes with the HDX relay mechanism. Alternatively, additional exchange may occur but is extremely slow and not observed on the time scale and pressure regime of this experiment. Although it is not clear which H is exchanging for D in the DabA b_2^+ ion (perhaps the hydroxyl H of the

dx.doi.org/10.1021/jp300262d | J. Phys. Chem. A 2012, 116, 4296−4304

hydroxyimine), the dominant exchange of only one H in this ion is consistent with structures that lack protonation at the amino side chain, as shown in Figure 6b.

To further probe the influence of the length and relative position of the side chain nitrogen in linear, alkylamine side chains, the KA b_2^+ ion structure was also studied. The action IRMPD spectrum and theoretical IR spectra for the oxazolone, side chain-ring, and diketopiperazine structures of the KA b_2^+ are shown in Figure 8. Two lowest-energy diketopiperazine

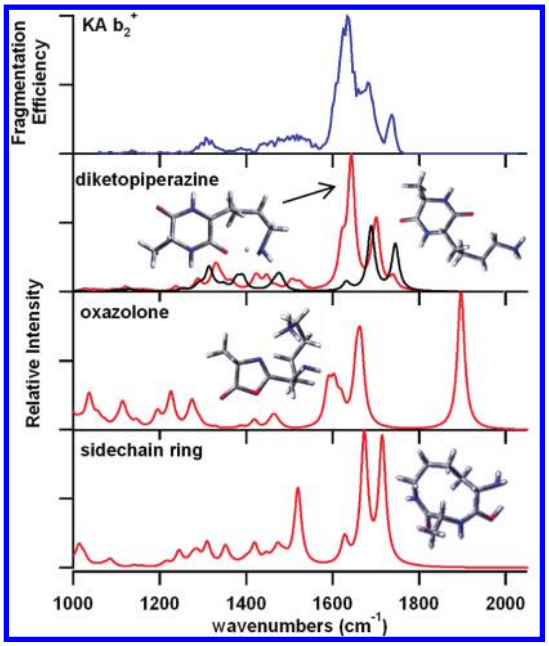

Figure 8. Action IRMPD spectrum of the KA b_2^+ ion generated from the KAAAA protonated precursor. Corresponding theoretical diketopiperazine, oxazolone, and side chain ring structure theoretical spectra, generated from the lowest-energy calculated structures, are shown for comparison. Two diketopiperazine structures are shown (lowest energy structure corresponds to curve indicated by the arrow), as both are expected to contribute to the overall spectrum.

structures are seen to contribute to the overall IR spectrum: while both structures are protonated on the side chain amine, the lowest energy structure bridges the proton with the diketopiperazine carbonyl oxygen, while the other structure features the protonated amine rotated away from the rest of the diketopiperazine ring. As the side chain amine may also act as a nucleophile, similar to the N-terminal amine, the side chain-cyclized system was calculated for both the KA and DabA b_2^+ ion systems. In comparison with Dab, lysine features two additional methylene carbons in the side chain between the amine group and peptide backbone, which may offer additional flexibility to allow the side chain to more readily bridge with the rest of the b_2^+ ion structure, making HDX via the relay mechanism more facile. Similar to DabA, the IRMPD spectrum features stretches indicative of only a diketopiperazine structure with no measured oxazolone contribution. The HDX behavior, shown in Figure 7b, is clearly different from that of Dab with four total hydrogens exchanging. In accord with other observed diketopiperazine structures that contain a basic side chain, a D_1 population appears after long exchange times (30 s), after the initial D_1 corresponding to the rapid incorporation of the other three deuterium atoms disappears. Of the four total exchanging hydrogens, three can likely be attributed to the three hydrogens on the protonated lysine side chain. In comparison to Dab, the increased side chain length in lysine facilitates bridging with CD_3OD more effectively, allowing the exchange of the side chain hydrogens to be observed within the time scale and pressure conditions of the FTICR HDX experiment.

As four total deuterium atoms are observed to incorporate into the KA b_2^+ ion structure, the fourth deuterium must be incorporated at a backbone amide nitrogen location. KA is the first example of a b_2^+ ion system that requires for the HDX behavior to include exchange at an amide hydrogen location, if only the side chain protonated diketopiperazine is considered. Again, similar to structural behavior displayed by DabA, a carbonyl-protonated hydroxyimine isomer would provide protonation sites of similar basicity to allow for the exchange of all four deuterium atoms. However, the structure of the hydroxyimine tautomer does not match the experimental IR spectrum observed for the KA b_2^+ ion. While the hydroxyimine is not observed in the action IRMPD experiment, the insertion of a deuterated methanol molecule may allow for the stabilization of the hydroxyimine tautomer and involvement of that structure during the exchange experiment.

While the side chain nitrogens in both 4-(pa) and lysine are the same distances away from the peptide backbone, KA exclusively forms the diketopiperazine, whereas 4-(pa)A exclusively forms oxazolone b_2^+ ions. These findings suggest that the presence of the ring structure in the side chain of the 4-(pa) residue introduces a steric hindrance that inhibits diketopiperazine formation. By comparison, the presence of the ring then favors oxazolone formation. However, additional factors beyond the presence or absence of a ring have already been shown to contribute to the formation of either the oxazolone or diketopiperazine structure.

A summary of the lowest-energy diketopiperazine, oxazolone, and, when applicable, side chain ring structures are summarized in Table 1. Without exception, a diketopiperazine structure is

Table 1. Summary of Relative Zero-Point Corrected Total Energies (in kJ/mol) of Structures for Histidine Analogue-Containing b_2^+ Ions Calculated at the 6-311++G Level**

b_2^+ ion	oxazolone	diketopiperazine	side chain ring
HA	85.7	0.0	
π-methyl-HA	71.7	0.0	
τ-methyl-HA	85.3	0.0	
(2-pa)A	78.2	0.0, 11.7	
(3-pa)A	70.9	0.0	
(4-pa)A	71.0	0.0	
DabA[a]	88.1	0.0 (side chain)	100.6
	0.0	12.1, 27.4 (carbonyl)	
KA	77.5	0.0, 0.5	86.3
(4-ta)A	74.9	0.0	

[a]The DabA carbonyl-protonated diketopiperazine is higher in energy than the lowest energy side chain protonated diketopiperazine as well as the lowest energy oxazolone structure (see text for explanation).

the thermodynamically favored product for each of the peptide b_2^+ ions studied. (In the case of DabA, while the side chain protonated diketopiperazine is the lowest-energy structure, a higher energy, amide-protonated hydroxyimine is in better agreement with the experimental spectrum.) Despite energetic considerations, oxazolone structures are observed for several b_2^+ ion systems, suggesting that energetic arguments alone are insufficient to determine the preferential ion structure(s) that

dx.doi.org/10.1021/jp300262d | J. Phys. Chem. A 2012, 116, 4296−4304

will be formed during the dissociation process, and that the reaction may produce the kinetically favored product in some cases. Compared with some systems reported in the literature, such as AG or AA, the differences in energy between the oxazolone and diketopiperazine isomers for the systems in the present work are quite large.

Theoretical work performed by Paizs and co-workers on the GGG system explored the different pathways involved in the formation of oxazolone versus diketopiperazine b_2^+ ion structures.[42,50] Their theoretical results suggest that preferential formation of oxazolone or diketopiperazine b_2^+ ion structure depends on the cis or trans conformation of the first peptide bond. If in the trans conformation, as typical for most peptide bonds, the geometry of the peptide preferentially favors the oxazolone formation. If the first peptide bond is in the cis conformation, the conformation facilitates diketopiperazine formation. Paizs and co-workers proposed that trans−cis isomerization of the first peptide bond relies on the transfer of the ionizing proton to the nitrogen of the amide bond. When protonation occurs, the double bond character of the peptide bond is lost, allowing for rotation of the now single bond to the cis conformation.

While certain residues, such as proline, have a greater percentage of peptide bonds in the cis conformation than other residues, peptide bonds are much more often found in the trans conformation (1000:1) with Pro favoring trans over cis only by 3:1.[51] Therefore, in order for a diketopiperazine structure to form, a trans−cis isomerization must occur, as proposed by Paizs and co-workers. On the basis of the results seen for the histidine analogue-containing b_2^+ ions, we propose that the availability of protonated histidine π-nitrogen, or other appropriate protonated side chain nitrogens such as those found in the Dab and Lys, facilitates the formation of the diketopiperazine structure by providing a protonated nitrogen in a location that can allow for proton transfer or bridging to the nitrogen (or perhaps carbonyl oxygen as proposed above for Dab) of the XxxAla amide bond, thus also facilitating the isomerization. Additionally, we propose that some feature(s) of the HisAla and 2(pa)A systems inhibit complete isomerization, allowing for the oxazolone pathway to still proceed; this explains why a mixture of structures is present for the HA b_2^+ ion. Linear side chains like DabA and KA form the diketopiperazine b_2^+ exclusively, suggesting that the trans−cis isomerization can proceed more readily in these cases. One contrast between HA and 2(pa)A versus DabA and KA is the dihedral angle involving the basic N, with greater angles for His and 2(pa), perhaps leading to less favorable proton bridging to initiate the trans−cis isomerization. Additionally, the location of the side chain nitrogen in relation to the peptide backbone, not only the existence of a side chain nitrogen, is essential for the proton transfer site to be in such a position to facilitate trans−cis isomerization and subsequently form the diketopiperazine structure, with no diketopiperazine formed by the 3(pa) and 4(pa) analogues. In the HA system, the availability and accessibility of the histidine π-nitrogen is essential for and stabilizes the formation of the diketopiperazine b_2^+ ion. However, as demonstrated by many of the analogue systems, diketopiperazine formation is possible in the absence of a true π-nitrogen or a side chain ring. The presence and appropriate position of a protonation site on the first residue's side chain allows formation, and perhaps subsequent stabilization of, the cis conformation of the peptide bond to allow for diketopiperazine formation.

CONCLUSIONS

A series of histidine side chain analogues have been studied to elucidate which structural features of an amino acid side chain contribute to the preferential formation of either the oxazolone and/or diketopiperazine b_2^+ ion structure. The presence of a basic side chain allows for facile conversion of the first peptide bond to the cis conformation, which puts the peptide in a conformation that readily allows for diketopiperazine formation. In addition to the presence of the basic side chain, the position of the side chain nitrogen is also essential for diketopiperazine formation. The small amount of oxazolone produced for HA and 2(pa)A is consistent with a population of ions that fragments directly from the trans precursor without a trans−cis isomerization event. Additionally, the IRMPD spectroscopy and hydrogen−deuterium exchange results suggest that MS/MS information alone is insufficient to predict a peptide fragment ion structure. For the similar system HG and GH studied by the O'Hair laboratory, theory and MS/MS fragmentation patterns predicted the structures of those b_2^+ ions to be diketopiperazines.[30] However, in the very similar HA system, a mixture of the two structures is seen. Future computational studies modeling the rotational barrier between the trans and cis conformations of the first peptide bond for these histidine and histidine-analogue-containing peptides should prove to be extremely useful in fully understanding the mechanism of b_2^+ ion formation for these peptide systems; modeling of the cis−trans rotational barrier for the DabA system, with the smaller ethylamine side chain, may be most computationally feasible and has been initiated in our lab. While additional insight into the histidine system has been obtained as a result of these studies, the structural analogues provided numerous examples showing that peptides containing any one of the several basic residues are capable of forming diketopiperazine structures. Examination of less basic "proton carrier" side chains such as those in glutamine and asparagine is underway to determine if they can also assist diketopiperazine formation.

ASSOCIATED CONTENT

Supporting Information

HA b_2^+ ion structures and spectra, as well as magnified structures and coordinates for all calculated b_2^+ ions. This material is available free of charge via the Internet at http://pubs.acs.org.

AUTHOR INFORMATION

Corresponding Author

*Phone: (520) 621-2628. Fax: (520) 621-8407. E-mail: vwysocki@email.arizona.edu.

Present Address

[§]Division of Pharmaceutical Analysis, U.S. FDA, 1114 Market Street, St. Louis, Missouri 63101, United States. E-mail: ashley.gucinski@fda.hhs.gov.

Notes

The authors declare no competing financial interest.

ACKNOWLEDGMENTS

Funding from NIH GMR0151387 awarded to V.H.W. is gratefully acknowledged. We gratefully acknowledge the aid, expertise, and provision of CLIO beam time from the CLIO staff, including P. Maître, V. Steinmetz, J. Lemaire, R. Sinha, B. Rieul, and C. Six. We thank A. Gelb for assistance with peptide

synthesis. The research leading to these results has received funding from the European Union's Seventh Framework Programme (FP7/2007-2013) under grant agreement no. 226716.

REFERENCES

(1) Roepstorff, P. *Biomed. Mass Spectrom.* **1984**, *11*, 601.
(2) Elias, J. E.; Gibbons, F. D.; King, O. D.; Roth, F. P.; Gygi, S. P. *Nat. Biotechnol.* **2004**, *22*, 214−219.
(3) Nesvizhskii, A. E.; Vitek, O.; Aebersold, R. *Nat. Methods* **2007**, *4*, 787−797.
(4) Perkins, D. N.; Pappin, D. J.; Creasy, D. M.; Cottrell, J. S. *Electrophoresis* **1999**, *20*, 3551−3567.
(5) Bleiholder, C.; Osburn, S.; Williams, T. D.; Suhai, S.; Van Stipdonk, M.; Harrison, A. G.; Paizs, B. *J. Am. Chem. Soc.* **2008**, *130*, 17774−17789.
(6) Gucinski, A. C.; Somogyi, A.; Chamot-Rooke, J.; Wysocki, V. H. *J. Am. Soc. Mass Spectrom.* **2010**, *21*, 1329−1338.
(7) Harrison, A. G.; Yalcin, T. *Int. J. Mass Spectrom.* **1997**, 165.
(8) Ballard, K. D.; Gaskell, S. J. *J. Am. Soc. Mass Spectrom.* **1993**, *4*, 477−481.
(9) Li, W.; Ji, L.; Goya, J.; Tan, G.; Wysocki, V. *J. Proteome Res.* **2011**, *10*, 1593−1602.
(10) Breci, L. A.; Tabb, D. L.; Yates, J. R., III; Wysocki, V. *Anal. Chem.* **2003**, *75*, 1963−1971.
(11) Bythell, B. J.; Knapp-Mohammady, M.; Paizs, B.; Harrison, A. G. *J. Am. Soc. Mass Spectrom.* **2010**, *21*, 1352−1363.
(12) Gu, C.; Tsaprailis, G.; Breci, L.; Wysocki, V. H. *Anal. Chem.* **2000**, *72*, 5804−5813.
(13) Herrmann, K. A.; Wysocki, V. H.; Vorpagel, E. R. *J. Am. Soc. Mass Spectrom.* **2005**, *16*, 1067−1080.
(14) Paizs, B.; Suhai, S. *Mass Spectrom. Rev.* **2005**, *24*, 508−548.
(15) Perkins, B. R.; Chamot-Rooke, J.; Yoon, S. H.; Gucinski, A. C.; Somogyi, A.; Wysocki, V. *J. Am. Chem. Soc.* **2009**, *131*, 17528−17529.
(16) Tsaprailis, G.; Nair, H.; Somogyi, A.; Wysocki, V. H.; Zhong, W. Q.; Futrell, J. H.; Summerfield, S. G.; Gaskell, S. J. *J. Am. Chem. Soc.* **1999**, *121*, 5142−5154.
(17) Tsaprailis, G.; Nair, H.; Zhong, W.; Kuppanan, K.; Futrell, J. H.; Wysocki, V. H. *Anal. Chem.* **2004**, *76*, 2083−2094.
(18) Tsaprailis, G.; Somogyi, A.; Nikolaev, E. N.; Wysocki, V. H. *Int. J. Mass Spectrom.* **2000**, *195/196*, 467−479.
(19) Dongre, A. R.; Jones, J. L.; Somogyi, A.; Wysocki, V. *J. Am. Chem. Soc.* **1996**, *118*, 8365−8374.
(20) Nair, H.; Somogyi, A.; Wysocki, V. H. *J. Mass Spectrom.* **1996**, *31*, 1141−1148.
(21) Schnier, P. D.; Price, W. D.; Jockusch, R. A.; Williams, E. R. *J. Am. Chem. Soc.* **1996**, *118*, 7178−7189.
(22) Summerfield, S. G.; Whiting, A.; Gaskell, S. J. *Int. J. Mass Spectrom. Ion Processes* **1997**, *162*, 149−161.
(23) Tang, X. J.; Thibault, P.; Boyd, R. K. *Anal. Chem.* **1993**, *65*, 2824−2834.
(24) Vachet, R. W.; Asam, M. R.; Glish, G. L. *J. Am. Chem. Soc.* **1996**, *118*, 6252−6256.
(25) Vaisar, T.; Urban, J. *J. Mass Spectrom.* **1998**, *33*, 505−524.
(26) Wu, Q.; Van Orden, S.; Cheng, X.; Bakhtiar, R.; Smith, R. D. *Anal. Chem.* **1995**, *67*, 2498−2509.
(27) Wyttenbach, T.; von Helden, G.; Bowers, M. T. *J. Am. Chem. Soc.* **1996**, *118*, 8355−8364.
(28) Tabb, D. L.; Smith, L. L.; Breci, L. A.; Wysocki, V. H.; Lin, D.; Yates, J. R. *Anal. Chem.* **2003**, *75*, 1155−1163.
(29) Reimer, U.; El Mokdad, N.; Schutkowski, M.; Fischer, G. *Biochemistry* **1997**, *36*, 13802−13808.
(30) Farrugia, J. M.; Taverner, T.; O'Hair, R. A. J. *Int. J. Mass Spectrom.* **2001**, *209*, 99−112.
(31) Bythell, B. J.; Somogyi, A.; Paizs, B. *J. Am. Soc. Mass Spectrom.* **2009**, *20*, 618−624.
(32) Oomens, J.; Young, S.; Molesworth, S.; van Stipdonk, M. *J. Am. Soc. Mass Spectrom.* **2009**, *2009*, 334−339.
(33) Yoon, S. H.; Chamot-Rooke, J.; Perkins, B. R.; Hilderbrand, A. E.; Poutsma, J. C.; Wysocki, V. H. *J. Am. Chem. Soc.* **2008**, *130*, 17644−17645.
(34) Chen, X.; Yu, L.; Steill, J.; Oomens, J.; Polfer, N. C. *J. Am. Chem. Soc.* **2009**, *131*, 18273−18282.
(35) Polfer, N. C.; Oomens, J.; Suhai, S.; Paizs, B. *J. Am. Chem. Soc.* **2007**, 129.
(36) Woodin, R. L.; Bomse, D. S.; Beauchamp, J. L. *J. Am. Chem. Soc.* **1978**, *100*, 3248−3250.
(37) Atherton, E.; Sheppard, R. C. *Solid-Phase Peptide Synthesis: A Practical Approach*; Oxford University Press: Oxford, U.K., 1989.
(38) Lemaire, J.; Boissel, P.; Heninger, M.; Mauclaire, G.; Bellec, G.; Mestdagh, H.; Simon, A.; Le Caer, S.; Ortega, J. M.; Glotin, F.; Maitre, P. *Phys. Rev. Lett.* **2002**, *89*, 273002/273001−273002/273004.
(39) Mac Aleese, L.; Simon, A.; McMahon, T. B.; Ortega, J.; Scuderi, D.; Lemaire, J.; Maitre, P. *Int. J. Mass Spectrom.* **2006**, *249*−*250*, 14−20.
(40) Maitre, P.; Le Caer, S.; Simon, A.; Jones, W.; Lemaire, J.; Mestdagh, H.; Heninger, M.; Mauclaire, G.; Boissel, P.; Prazeres, R.; Glotin, F.; Ortega, J. M. *Nucl. Instrum. Methods Phys. Res., Sect. A* **2003**, *507*, 541−546.
(41) Frisch, M. J.; Trucks, G. W.; Schlegel, H. B.; Scuseria, G. E.; Robb, M. A.; Cheeseman, J. R.; Scalmani, G.; Barone, V.; Mennucci, B.; Petersson, G. A.; Nakatsuji, H.; Caricato, M.; Li, X.; Hratchian, H. P.; Izmaylov, A. F.; Bloino, J.; Zheng, G.; Sonnenberg, J. L.; Hada, M.; Ehara, M.; Toyota, K.; Fukuda, R.; Hasegawa, J.; Ishida, M.; Nakajima, T.; Honda, Y.; Kitao, O.; Nakai, H.; Vreven, T.; Montgomery, J. A., Jr.; Peralta, J. E.; Ogliaro, F.; Bearpark, M.; Heyd, J. J.; Brothers, E.; Kudin, K. N.; Staroverov, V. N.; Kobayashi, R.; Normand, J.; Raghavachari, K.; Rendell, A.; Burant, J. C.; Iyengar, S. S.; Tomasi, J.; Cossi, M.; Rega, N.; Millam, J. M.; Klene, M.; Knox, J. E.; Cross, J. B.; Bakken, V.; Adamo, C.; Jaramillo, J.; Gomperts, R.; Stratmann, R. E.; Yazyev, O.; Austin, A. J.; Cammi, R.; Pomelli, C.; Ochterski, J. W.; Martin, R. L.; Morokuma, K.; Zakrzewski, V. G.; Voth, G. A.; Salvador, P.; Dannenberg, J. J.; Dapprich, S.; Daniels, A. D.; Farkas, O.; Foresman, J. B.; Ortiz, J. V.; Cioslowski, J.; Fox, D. J. *Gaussian 09*, revision A.01; Gaussian, Inc.: Wallingford, CT, 2009.
(42) Paizs, B.; Suhai, S. *Rapid Commun. Mass Spectrom.* **2001**, *15*, 2307−2323.
(43) Yalcin, T.; Khouw, C.; Csizmadia, I. G.; Peterson, M. R.; Harrison, A. G. *J. Am. Soc. Mass Spectrom.* **1995**, *7*, 233−242.
(44) Perkins, B. R. The University of Arizona, *Gaussian 09*, revision A.01, 2009.
(45) Wysocki, V. H.; Tsaprailis, G.; Smith, L. L.; Breci, L. A. *J. Mass Spectrom.* **2000**, *35*, 1399−1406.
(46) Lucas, B.; Gregoire, G.; Lemaire, J.; Maitre, P.; Glotin, F.; Schermann, J. P.; Desfrancois, C. *Int. J. Mass Spectrom.* **2005**, *243*, 105−113.
(47) Campbell, S.; Rodgers, M. T.; Marzluff, E. M.; Beauchamp, J. L. *J. Am. Chem. Soc.* **1994**, *116*, 9765−9766.
(48) Campbell, S.; Rodgers, M. T.; Marzluff, E. M.; Beauchamp, J. L. *J. Am. Chem. Soc.* **1995**, *117*, 12840−12854.
(49) Gucinski, A. C.; Chamot-Rooke, J.; Steinmetz, V.; Somogyi, A.; Wysocki, V. H. Manuscript in preparation.
(50) Paizs, B.; Suhai, S. *Rapid Commun. Mass Spectrom.* **2002**, *16*, 375−389.
(51) Pal, D.; Chakrabarti, P. *J. Mol. Biol.* **1999**, *294*, 271−288.